

Journal of Materials Chemistry A

Accepted Manuscript



This is an *Accepted Manuscript*, which has been through the Royal Society of Chemistry peer review process and has been accepted for publication.

Accepted Manuscripts are published online shortly after acceptance, before technical editing, formatting and proof reading. Using this free service, authors can make their results available to the community, in citable form, before we publish the edited article. We will replace this *Accepted Manuscript* with the edited and formatted *Advance Article* as soon as it is available.

You can find more information about *Accepted Manuscripts* in the [Information for Authors](#).

Please note that technical editing may introduce minor changes to the text and/or graphics, which may alter content. The journal's standard [Terms & Conditions](#) and the [Ethical guidelines](#) still apply. In no event shall the Royal Society of Chemistry be held responsible for any errors or omissions in this *Accepted Manuscript* or any consequences arising from the use of any information it contains.

One pot synthesis of Nickel foam supported self-assembly of NiWO₄, CoWO₄ nanostructures that act as high performance electrochemical capacitor electrodes

Guanjie He^a, Jianmin Li^b, Wenyao Li^c, Bo Li^d, Nuruzzaman Noor^a, Kaibing Xu^b, Junqing Hu^{b*} and Ivan P. Parkin^{a*}

^a*Materials Chemistry Centre, Department of Chemistry, University College London, 20 Gordon Street, London WC1H 0AJ, U.K., E-mail: i.p.parkin@ucl.ac.uk*

^b*State Key Laboratory for Modification of Chemical Fibers and Polymer Materials, College of Materials Science and Engineering, Donghua University, Shanghai 201620, China. E-mail: hu.junqing@dhu.edu.cn*

^c*School of Material Engineering, Shanghai University of Engineering Science, Shanghai 201620, China*

^d*Department of Chemistry, Duke University, NC 27708, U.S.A.*

Abstract

In this work, we report a facile one-step hydrothermal approach to synthesize NiWO₄ and CoWO₄ nanostructures on nickel foam as the binder-free electrodes for use as supercapacitors. The as-synthesized materials showed excellent electrochemical performance, with a high specific capacitance of 797.8 F g⁻¹ and 764.4 F g⁻¹ at a

current density of 1 A g^{-1} after 3000 cycles, increasing the current density by 20 times, the rate capabilities still maintaining 55.6% and 50.6% of the original value for NiWO_4/Ni foam and CoWO_4/Ni foam, respectively. Moreover, both of these materials exhibited outstanding cycling stability, the 6000th cycle at 50 mV s^{-1} demonstrated 2.06 and 2.81 times, better capacitance than the initial cycles for NiWO_4/Ni foam and CoWO_4/Ni foam, respectively. To our knowledge, this capacitance performance is better than any previously reported for these materials and is a consequence of the highly evolved surface area/microstructure of the materials formed by this technique.

Introduction

In order to satisfy the increasing demands for energy, many energy storage devices have been explored and intensively developed. Much attention has been paid to supercapacitors, also known as the electrochemical capacitors (ECs) in recent years due to their outstanding and unique abilities such as fast charge-discharge rate, high power density and long-cycle lifespan.¹ Based on their different charge storage mechanisms, supercapacitors can be classified into two groups: electrical double layer capacitors (EDLCs) and pseudocapacitors (PCs). EDLCs, carbon-based nanomaterials for example, store electrical energy *via* reversible ion-absorption at the interface of electrode and electrolyte. Compared with EDLCs, PCs exhibit higher specific capacitance and energy density, which are attributed to the fast reversible redox reactions between the different valence states of the transition metal oxide used as the electrode. Much effort has been focused on transition metal oxide (TMO) for PCs

applications, such as NiO,^{2,3} Co₃O₄,⁴ MnO₂,⁵ WO₃,⁶ and V₂O₅.⁷ However, the poor electrical conductivity and the rapid decline of the capacitance for most binary metal oxides are the big hurdles to their practical applications. Ternary transition metal oxides with two different metal cations are promising electrode candidates for energy-storage applications. The combination of two different metal cations could enhance the conductivity greatly or provide a wide range of oxidation states in comparison with their individual binary oxide counter parts thus potentially enabling improvements in electrochemical properties. Accordingly, various ternary transition metal oxides with controlled morphologies have been synthesized and achieved better electrochemical performance, such as NiCo₂O₄,^{8,9} CoMoO₄,¹⁰ NiMoO₄,¹¹ and CoMn₂O₄.¹² Currently, the design and synthesis of novel ternary transition metal oxides nanomaterials with superior electrochemical properties is still a key area of research. Another method to enhance the conductivity could be exchanging O by S.^{13,14} Compared with metal sulfides, tungstates materials possess easy preparation method, low price, low toxicity and stable multifunctional properties.¹⁵⁻¹⁷ Importantly, tungstates materials presents high conductivity, higher than most binary and some ternary metal oxides. As reported in some literatures, nickel tungstate (NiWO₄) presents a conductivity on the order of 10⁻⁷-10⁻² S cm⁻¹, much higher than NiO (10⁻¹³ S cm⁻¹)^{18,19} and NiMoO₄ (10⁻¹¹-10^{-4.5} S cm⁻¹)^{20,21}, Because of the various valence states of W,²² which can be used for taking part in redox reactions for PC electrodes Nickel tungstate (NiWO₄) and cobalt tungstate (CoWO₄) have been investigated as promising candidates for catalysis.^{23,24} However, reports related to utilizing them as

the new type supercapacitor electrodes are scarce. Niu et al.¹⁸ prepared amorphous NiWO₄ nanostructures *via* a co-precipitation method. They explored the influence of synthesis temperature on the specific capacitance. The highest specific capacitance for NiWO₄ nanostructures was 586.2 F g⁻¹ at 0.5 A g⁻¹. They indicated that the NiWO₄ showed great conductivity enhancement due to the incorporation of W atoms compared with NiO. Ye et al.²⁵ used the hydrothermal method to prepare CoWO₄ on reduced graphene oxide as supercapacitors, which achieved a specific capacitance of 159.9 F g⁻¹ at 5 mV s⁻¹ calculated from CV curves and a capacitance retention of ~94.7% after 1000 cycles. Despite these efforts, synthesis of NiWO₄ and CoWO₄ based electrodes by a simple method and furthermore improving their electrochemical properties are still great challenges. Nowadays, a promising strategy has been developed to synthesize electroactive materials on the current collectors directly as binder-free electrodes. This strategy avoids the complicated electrodes making process for powdery samples, more importantly, it can greatly enhance the electron conductivity enabling more electroactive materials to be in good contact with the electrolyte to participate in the Faradaic reactions for energy storage, thus enormously improving their electrochemical performance.²⁶⁻²⁸

In this work, for the first time, we used an easily-controlled one-pot hydrothermal method to directly synthesize NiWO₄ and CoWO₄ nanostructures on Ni-foam as the binder-free electrodes for PCs. Their electrochemical properties were fully explored and compared with their powdery samples analogues. It was demonstrated that these binder-free electrode exhibits high specific capacitance (797.8 F g⁻¹ for NiWO₄/Ni

foam and 764.4 F g^{-1} for CoWO_4/Ni foam at the current density of 1 A g^{-1} , respectively), outstanding rate capability (55.6% for NiWO_4/Ni foam and 50.6% and CoWO_4/Ni foam, respectively, with a current density increase of 20 times) and excellent cycling stability (more than 200% of their initial specific capacitance after 6000 cycles). Compared with other reported NiWO_4 , CoWO_4 nanostructures as the electrodes for supercapacitors, our NiWO_4/Ni foam and CoWO_4/Ni foam nanostructures showed superior electrochemical properties. It is proposed that these two Ni foam supported nanostructures could be used as candidates for supercapacitor electrodes.

Experimental Sections

Materials Synthesis. The chemicals were purchased from Sigma (U.K.) and Sinopharm Chemical Reagent Co. (Shanghai, China), they were of analytical grade and used without further purification. In a typical synthesis, 0.291 g of $\text{Ni}(\text{NO}_3)_2 \cdot 6\text{H}_2\text{O}$ (or 0.291 g of $\text{Co}(\text{NO}_3)_2 \cdot 6\text{H}_2\text{O}$ as the cobalt source) was dissolved in 40 mL of deionized water to form a light green (or pink) solution. 0.33 g of Na_2WO_4 was added to the above solutions and stirred for ~ 30 min. The Ni foam ($\sim 4 \text{ cm} \times 1 \text{ cm}$) as the current collector was immersed in 6 M hydrochloric acid for ~ 30 min under ultrasonic vibration to remove the oxide layer on its surface and washed with DI water for next step use. The $\text{Ni}^{2+}/\text{Co}^{2+}$, WO_4^{2-} solution was transferred into a 60 mL Teflon-lined stainless-steel autoclave with the Ni foam standing against the wall. The autoclaves were sealed and maintained in the furnace at $180 \text{ }^\circ\text{C}$ for 8 h. The autoclave

was cooled down to room temperature naturally and the final samples on the Ni foam were washed with deionized water and absolute ethanol successively and dried in a vacuum oven at 60 °C for 6 h.

Materials Characterization. As-prepared products were characterized by a scanning electron microscope (SEM; Hitachi S-4800), a transmission electron microscope (TEM; JEM-2100F) equipped with an energy dispersive X-ray spectrometer (EDX), a D/max-2550 PC X-ray diffractometer (XRD; Rigaku, Cu-K α radiation), an X-ray photoelectron spectroscopy (XPS; Thermo Scientific K-alpha photoelectron spectrometer), Raman Spectroscopy (Renshaw Raman microscope spectrometer with laser wavelength 488 nm). The mass of the electrode materials was weighed accurately by an XS analytical balance (Mettler Toledo; $\delta = 0.01$ mg).

Electrochemical Measurements. Electrochemical measurements of the as-synthesized electrodes were performed on an Autolab electrochemical workstation (PGSTAT302N) in a three-electrode cell with 2 M KOH as the electrolyte. A platinum (Pt) plate and an Ag/AgCl electrode were used as the counter and reference electrode, respectively. The Ni foam supported NiWO $_4$ or CoWO $_4$ nanostructures acted as the working electrode. The mass of the active materials on nickel foam is ~ 0.75 mg cm $^{-2}$ and ~ 2 cm 2 of the nickel foams are immersed in the electrolyte for testing.

Results and discussion

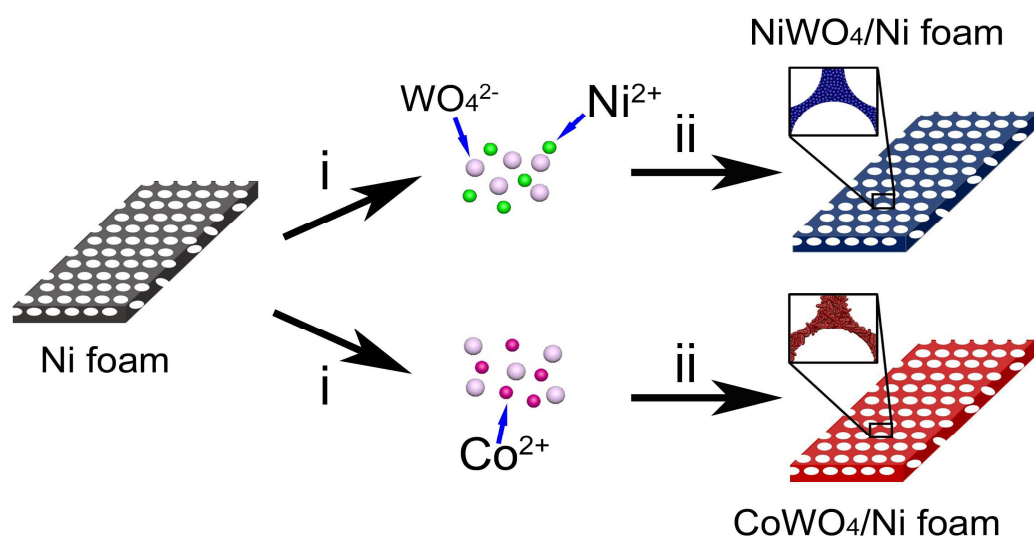


Figure 1. Schematic mechanism for the one-pot hydrothermal process of self-assembly $\text{NiWO}_4/\text{Ni foam}$ and $\text{CoWO}_4/\text{Ni foam}$ nanostructures.

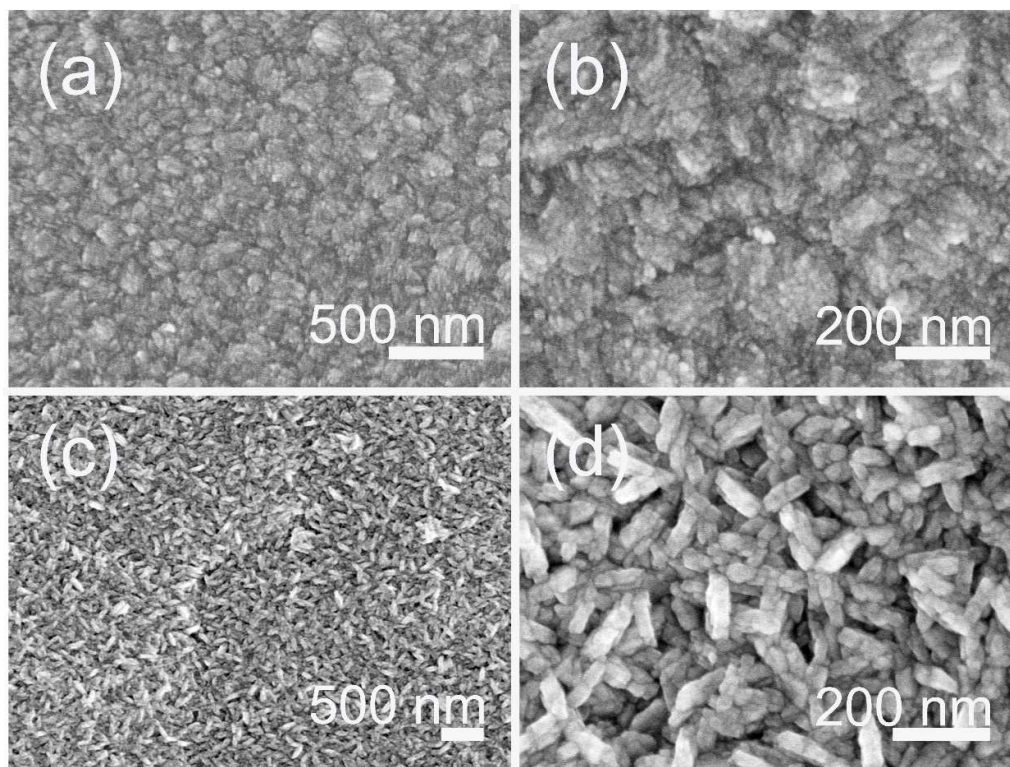


Figure 2 (a, b) Low and high magnification SEM image of as-synthesized NiWO₄ nanoparticles/Ni foam; (c, d) Low and high magnification SEM image of as-synthesized CoWO₄ nano-shuttles/Ni foam.

The NiWO₄/Ni foam and CoWO₄/Ni foam nanostructures were synthesized by the facile one-step hydrothermal method. The reaction system can be considered as a highly controllable and environmentally friendly for large scale and low-cost production of pseudocapacitors. The nanostructures (hill-shaped for NiWO₄ nanostructures and shuttle-like for CoWO₄ nanostructures) were self-assembled by the small individual nanoparticles and coated on the Ni foam to form a uniform coverage, as shown in Figure 1 and further demonstrated by the following analysis.

The morphologies of the as-synthesized materials were investigated by scanning electron microscopy (SEM). Commercial nickel foam still maintained its 3D porous structures after immersing in 6 M hydrochloric acid to remove the surface NiO layer and the hydrothermal reactions with the chemicals (Supplementary Figure S3a, b). Ni foam was utilized as the current collector directly because of its uniform macropore-structures providing a large support area and fast and efficient pathways for ion and electron transport for the active materials as well as excellent intrinsic electrical conductivity. Figure 2a and c are the low magnification SEM image of NiWO₄ and CoWO₄ nanostructures on nickel foam, respectively. Obviously, the nanostructures covered the Ni foam uniformly with no bare Ni foam being detected, as also can be demonstrated from lower magnification SEM (Supplementary Figure S3c, d). The NiWO₄ nanostructures exhibit hill-like hemisphere morphology composed of many small overlapped nanoparticles with the diameter of 100-200 nm, which can be demonstrated by high magnification SEM image in Figure 2b. Meanwhile, the high magnification SEM image of CoWO₄ nanostructures is shown in Figure 2d. CoWO₄ nanoparticles presented shuttle-like structures with rough surfaces, the length of which are ~100 nm and width of ~50 nm. As the electrodes for supercapacitors, both of their rough morphologies provide sufficient active sites for redox reactions and a huge surface area contacting with the electrolyte for the process of energy storage.

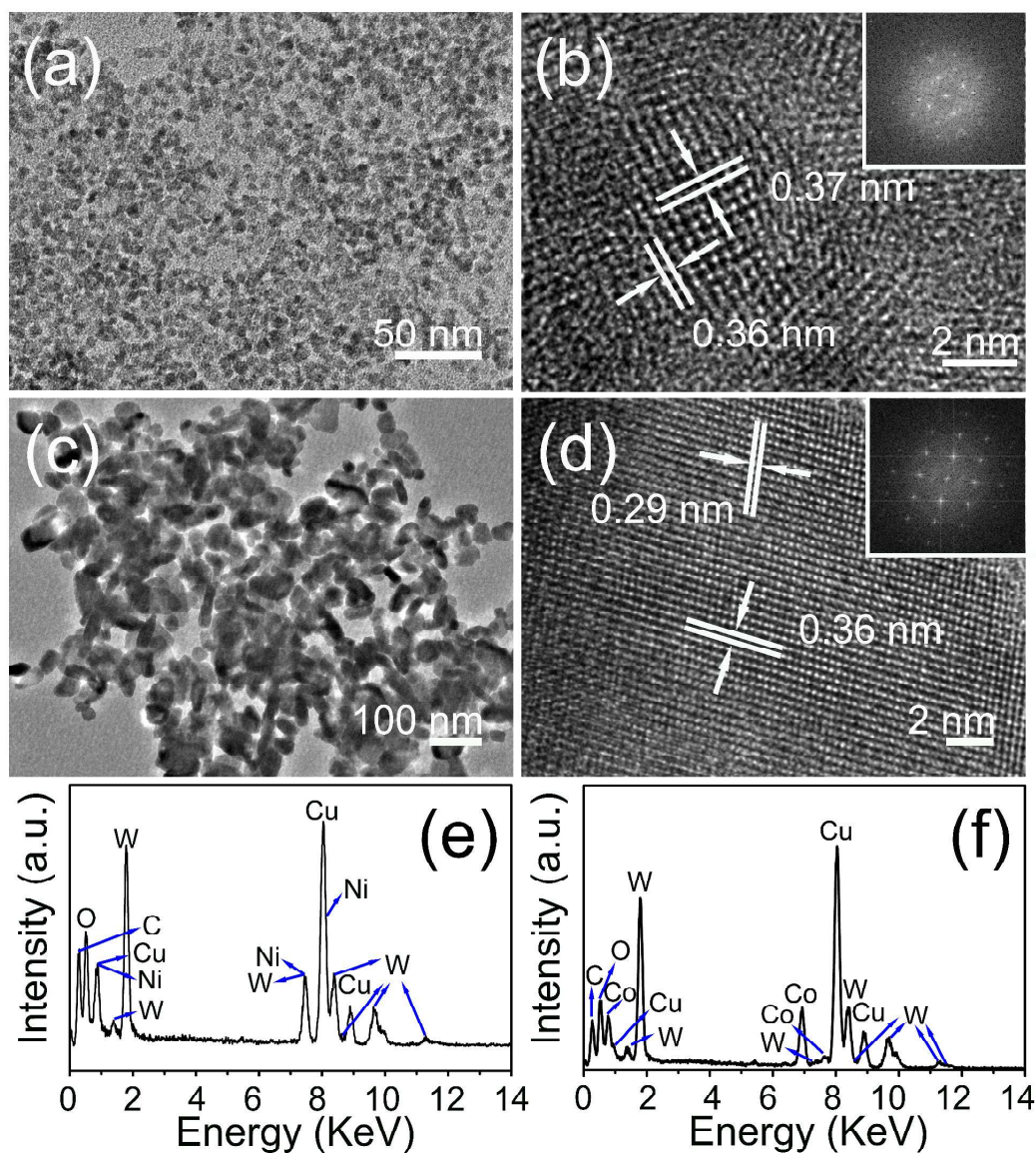


Figure 3 (a, b) TEM image and HRTEM of NiWO₄ nanostructures, respectively, inset is the corresponding FFT diffraction pattern; (c, d) TEM image and HRTEM of CoWO₄ nanostructures, respectively, inset is the corresponding FFT diffraction pattern; (e, f) EDX spectrum of NiWO₄ and CoWO₄ nanostructures, respectively.

The nanostructures and morphology of the samples were further investigated by

transmission electron microscopy (TEM) equipped with an energy dispersive X-ray spectrometer (EDX). The TEM samples were prepared through removing NiWO₄ and CoWO₄ structures from Ni foam by strong ultrasonic vibration in ethanol for ~30 min. Clearly, the large NiWO₄ hill-like nanostructures in SEM are composed of many tiny nanoparticles and the CoWO₄ shuttle-like nanostructures are constructed by lots of small nanoshuttles. Figure 3a and c are the typical TEM images of NiWO₄ and CoWO₄ nanoparticles, respectively. The diameters of individual nanoparticles are ~15 nm for NiWO₄ samples and the length of ~50 nm and the width of ~25 nm for CoWO₄ samples which can be corresponding to the rough morphology in the SEM samples, thus inducing the whole structures full of mesoporous. It is widely known the porous structures facilitate the mass-transport of electrodes within electrolytes for Faradaic redox reactions, which is also the critical issue for the electrolyte to contact with the active materials more efficiently. HRTEM of NiWO₄ nanostructures in Figure 3b showed clear lattice fringe with interplanar spacing (d-spacing) of 0.37 and 0.36 nm which are attributed to the {011}, {110} plane of the NiWO₄ crystal. The inset fast Fourier transformation (FFT) pattern from this image can be indexed as the [1 $\bar{1}$ 1] zone axis of the NiWO₄ monoclinic crystal. The HRTEM of CoWO₄ nanostructures are represented in Figure 3d, the d-spacing of 0.29 and 0.36 nm corresponds to the distance of the { $\bar{1}$ 11}, {011} facets of CoWO₄ crystals, an inset FFT pattern from this image can be indexed as the [01 $\bar{1}$] zone axis of the CoWO₄ monoclinic crystal. The EDX analysis (Figure 3e, f) also demonstrates the presence of Ni, W, O and Co, W, O elements; the Cu and C are from the TEM sample

carbon-copper grid.

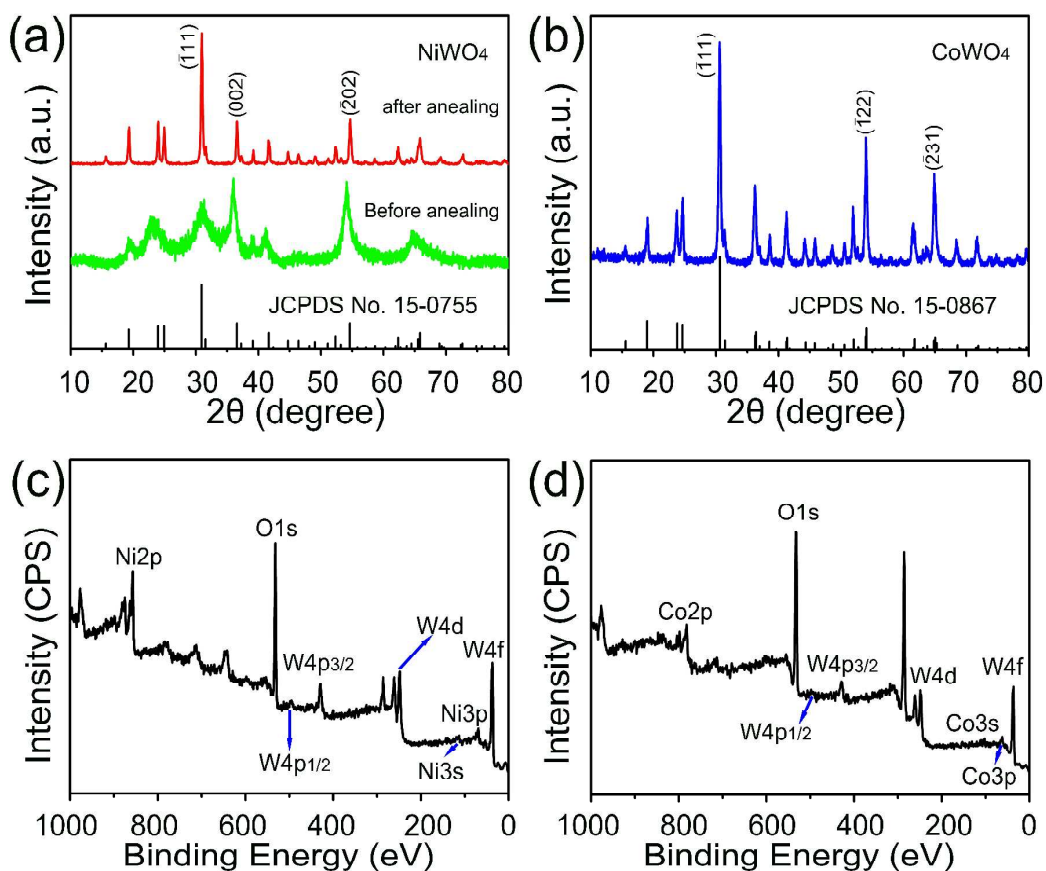


Figure 4 (a) XRD pattern of NiWO₄ nanostructures before (green line) and after (red line) annealing; (b) XRD pattern of CoWO₄ nanostructures; (c, d) XPS spectrum of NiWO₄/Ni foam and CoWO₄/Ni foam nanostructures, respectively.

The crystallographic phase of the NiWO₄/Ni foam and CoWO₄/Ni foam were further characterized by X-ray Diffraction (XRD). XRD samples were made by scratching the nanoparticles from the Ni foam in order to avoid the strong background of the Ni foam on XRD peak signals. The diffraction pattern of the standard NiWO₄ (JCPDS

card No. 15-0755) corresponds to that seen for the NiWO₄ nanostructures. Because of such small sizes of as-synthesized NiWO₄ nanostructures, this lead to broad and low intensity diffraction peaks. To get easily recognizable phase-distinguished samples, the NiWO₄ samples synthesized by hydrothermal methods were annealed at 600 °C for 1 h, XRD patterns were indexed to the standard pattern, furthermore, the Raman Spectrum (Supplementary Figure S4a) were an exact match for NiWO₄ after annealing. The CoWO₄ samples formed after hydrothermal system corresponded to the standard CoWO₄ structure (JCPDS card No. 15-0867) and Raman spectrum (Supplementary Figure S4b) were also in accordance with the literature.^{18,25} These techniques demonstrated that larger crystal structures of CoWO₄ samples compared to NiWO₄ only after the hydrothermal procedure. X-ray photoelectron spectroscopy (XPS) of NiWO₄ and CoWO₄ nanostructures are shown in Figure 4 c, d and Supplementary Figure S5. The survey scan spectrum shows the expected elements. Supplementary Figure S5 shows two major peaks with binding energies at 873.7 eV and 856.3 eV, agreeing well with the Ni 2p_{1/2} and Ni 2p_{3/2} spin-orbit peaks of the NiWO₄ phase, respectively,¹⁸ Co 2p_{1/2} and Co 2p_{3/2} peaks of Co can be detected in Supplementary Figure S5, O 1S and W 4p can be seen in the XPS of both samples. Moreover, the W 4f_{7/2} peaks at 35.8 eV combining with the Ni 2p_{3/2} peak at 856.3 eV for NiWO₄ nanostructures; the W 4f_{7/2} peak appearing at 35.5 eV with the Co 2p_{3/2} peak at 780.6 eV together for CoWO₄ samples suggest the formation of NiWO₄ and CoWO₄ binary metal oxide.^{18,25,29}

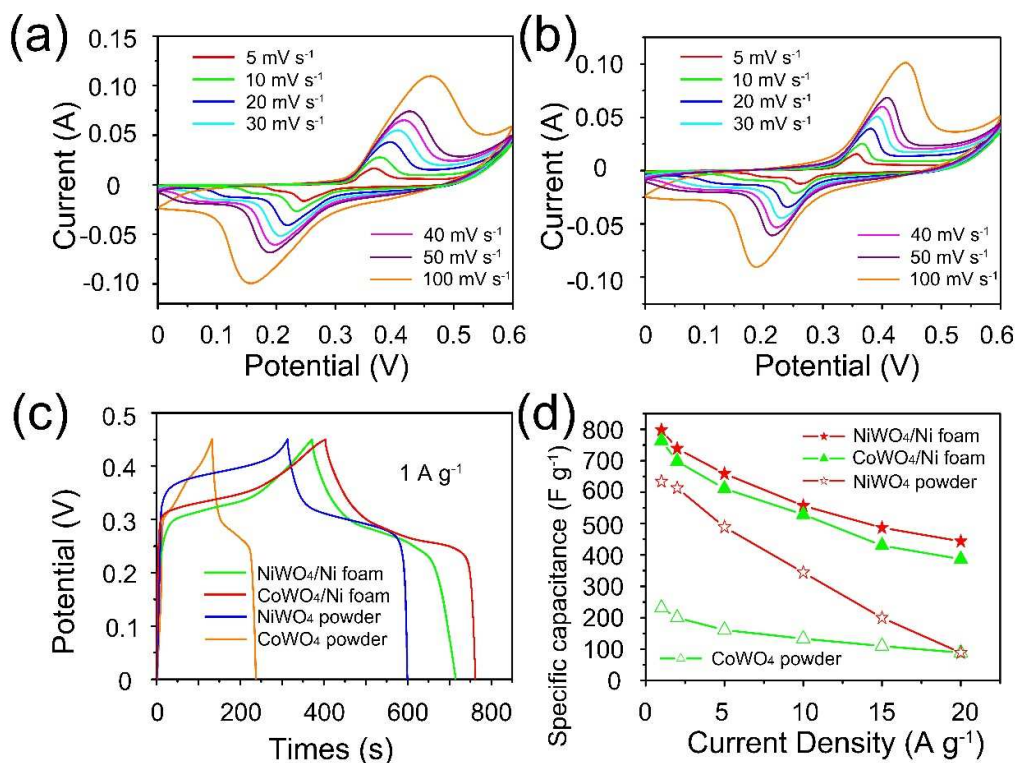


Figure 5 (a, b) cyclic voltammetry curves of the NiWO₄/Ni foam and CoWO₄/Ni foam at various scan rates, respectively. (c) A comparison of galvanostatic charge-discharge curves of NiWO₄/Ni foam, CoWO₄/Ni foam, NiWO₄ powder and CoWO₄ powder at a current density of 1 A g⁻¹. (d) A comparison of specific capacitances for NiWO₄/Ni foam, CoWO₄/Ni foam, NiWO₄ powder and CoWO₄ powder as a function of current density.

To explore the electrochemical performance of the as-synthesized electrodes, we carried out cyclic voltammetry (CV) and galvanostatic charge-discharge (CD) measurements on both by using NiWO₄/Ni foam, CoWO₄/Ni foam nanostructures and by fabricating their powdery samples onto the nickel foam as the working

electrodes in a three electrode test system with 2M KOH as the electrolyte (Procedure in Supplementary information). CV curves and CD curves for NiWO₄/Ni foam and CoWO₄/Ni foam nanostructures were investigated after 3000 cycles at 50 mV s⁻¹ for activation. From Figure 5 a and b, the CV curves at a series of scanning rates within the potential range of 0~0.6 V of the NiWO₄/Ni foam and CoWO₄/Ni foam respectively, strong redox peaks can be easily identified in each curve, which demonstrated the Faradic capacitive mechanism, i.e. reversible redox reactions between the Ni²⁺ and Ni³⁺ and the Co²⁺ and Co³⁺, respectively. From the Pourbaix diagram,²⁵ W does not take part in any redox reaction in the alkaline electrolyte and its role is to increase the conductivity of the whole active materials in the electrodes. Clearly, the shapes of the CV curves at different sweeping rates showed almost no change; the anodic peaks and cathodic peaks relating to oxidation and reduction processes shift to higher and lower potentials, respectively, due to faster ion and electron transport between the interface of active materials and electrolytes at higher scan rate. These phenomena indicated the excellent electrochemical reversibility of the synthesized electrodes. The comparison of the CD curves in a potential window between 0 and 0.45 V for NiWO₄/Ni foam and CoWO₄/Ni foam nanostructures, pure NiWO₄ and CoWO₄ powdery samples at the same current density of 1 A g⁻¹ are displayed in Figure 5c. It's well known that the galvanostatic charge-discharge measurement is an accurate method for estimating specific capacitance of pseudocapacitors by $C = \frac{It}{m\Delta V}$, where I (A) is the current applied for the charge-discharge, t (s) is the discharge time, m (g) is the weight of the active materials

in the electrodes, and ΔV (V) is the voltage interval of the discharge, the specific capacitance of NiWO₄ nanoparticles/Ni foam and CoWO₄ nanoshuttles/Ni foam are higher due to the longer discharging time compared with their powdery samples. The specific capacitance values are 797.8, 738.7, 658.9, 556.7, 486.7 and 443.6 F g⁻¹ for NiWO₄/Ni foam nanostructures and 764.4, 697.8, 611.1, 528.9, 430 and 386.7 F g⁻¹ for CoWO₄/Ni foam nanostructures at current densities of 1, 2, 5, 10, 15, 20 A g⁻¹, respectively, which were calculated from the discharge curves at different current densities (Supplementary Figure S6). The rate capability is an important parameter for power applications which reflects the retention of specific capacitance with increasing current density. Ni foam supported nanostructures possess much better rate capability compared with their powdery sample analogues, as shown in Figure 5d, which can be ascribed to the fact that Ni foam supported electrode materials exhibit more active reaction sites with the electrolyte to participate in the fast redox reactions and stronger adhesion with the current collector. The rate capabilities were 55.6% and 50.6% for NiWO₄ nanoparticles/Ni foam and CoWO₄ nanoshuttles/Ni foam, respectively, when the current density was increased by 20 times. These drops may be due to the incremental voltage drop and the fact that more active materials are not involved in the fast redox reaction with an increase in current density.

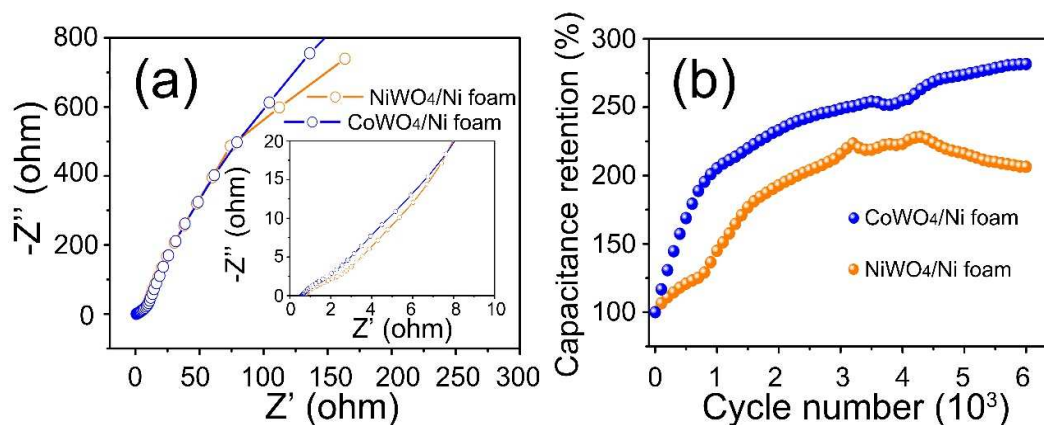


Figure 6 (a) EIS spectra of NiWO₄/Ni foam and CoWO₄/Ni foam nanostructures electrodes, inset shows the high frequency region of spectra; (b) Cycling performances of NiWO₄/Ni foam and CoWO₄/Ni foam nanostructures for 6000 cycles at 50 mV s⁻¹.

The electrical conductivity and ion-transfer ability of the supercapacitor working electrodes can be investigated by electrochemical impedance spectroscopy (EIS). Figure 6a shows the Nyquist plots of NiWO₄ and CoWO₄ nanostructures/Ni foam electrodes, respectively; and Supplementary Figure S7 described their equivalent fitting circuit. From the high frequency range, the inset of Figure 6 (a), equivalent series resistance (ESR) values, including inherent resistances of the active materials, bulk resistance of electrolyte and contact resistance of the interface between electrolyte and electrodes, are 0.575 and 0.515 Ω for NiWO₄/Ni foam and CoWO₄/Ni foam, respectively. Moreover, the open and free interspaces among these nanoparticles can act as an “ion storage” that can shorten the diffusion distance from the external electrolyte to the interior surfaces and thus minimize ion transport

resistance. Meanwhile, there is the semi-circle with an unclear arc in the high-frequency region, which can calculate the charge-transfer resistance (R_{ct}), reflecting the diffusion of electrons. The R_{ct} are 4.037 Ω of NiWO₄/Ni foam and 3.479 Ω of CoWO₄/Ni foam nanostructures, respectively. These parameters indicated that the good electrical conductivity and ion-diffusion behavior of as-synthesized electrodes, which are better than their parental binary metal oxides (NiO,³⁰ Co₃O₄,³¹ WO₃³²) nanostructures in the literature. The cycling stability is another critical parameter to measure the long-term performance of the supercapacitors for practical use. In our work, the cycling stability of the as-synthesized electrode materials was evaluated by repeating the CV test between 0 and 0.6 V at 50 mV s⁻¹ for 6000 cycles. Apparently, both of the specific capacitance of the two electrodes increased sharply in the first periods. This is due to the long activation period which can be ascribed to the rough morphology loaded with many tiny materials and it may take a long time to activate most of the active electrode materials. During this period, the electrode will be activated through the intercalation and de-intercalation of the ions from the electrolyte, thus contributing more active points to participate in the redox reactions. Interestingly, for both of the electrodes, there were further increases after some cycles' decline, which can be related to two reasons: (1) an improvement in the surface wetting of the electrode by the electrolyte during extended cycling;³³ (2) a small number of the nanoparticles dissolved during the cycling and the inner nanoparticles began to be activated. The specific capacitance after the 6000 cycles were 2.06 and 2.81 times of their first cycle for NiWO₄/Ni foam and CoWO₄/Ni foam

nanostructures, respectively. Impressively, the capacitance of CoWO₄/Ni foam nanostructures showed a rising trend even after 6000 cycles. The electrodes after cycling maintained their initial rough morphology after the long time duration of cycles (Supplementary Figure S8) which demonstrates the electrochemical properties and the structures are stable even after long-term cycling. The electrochemical performance of our Ni foam supported NiWO₄ and CoWO₄ nanostructures superior to other reported tungstate-based electrodes in the literature, as listed in Table 1.

Table 1 Comparison of electrochemical performance

Nanostructures	Specific capacitance	Cycling Stability (Compared with initial value)	Reference
NiWO ₄ /Ni foam nanostructures	797.8 F g ⁻¹ at 1 A g ⁻¹	2.06 times after 6000 cycles	Our work
CoWO ₄ /Ni foam nanostructures	764.4 F g ⁻¹ at 1 A g ⁻¹	2.81 times after 6000 cycles	Our work
NiWO ₄ amorphous nanostructure	586.2 F g ⁻¹ at 0.5 A g ⁻¹	0.9 times after 1000 cycles	18
CoWO ₄ /rGO nanocomposites	159.9 F g ⁻¹ at 5 mV s ⁻¹	0.947 times after 1000 cycles	25
NiWO ₄ DNA Scaffold	173 F g ⁻¹ at 5 mV s ⁻¹	0.9 times after 1000 cycles	34
WO ₃ /carbon aerogel composites	700 F g ⁻¹ at 25 mV s ⁻¹	0.95 times after 4000 cycles	35
ZrO ₂ -SiO ₂ /ultrasmall WO ₃ nanoparticles	313 F g ⁻¹ at 1 A g ⁻¹	0.9 times after 2500 cycles	36

Conclusion

In summary, an easily-controlled one-pot hydrothermal process was developed to synthesize NiWO₄ and CoWO₄ nanostructures on Ni foam with superior electrochemical properties for use as pseudocapacitors electrodes. The as-synthesized electrodes showed excellent electrochemical performance, such as a high specific

capacitance of 797.8 F g^{-1} and 764.4 F g^{-1} at the current density of 1 A g^{-1} after 3000 cycles; both of these materials exhibited outstanding cycling stability, the 6000th cycle at 50 mV s^{-1} were 2.06 and 2.81 times of their initial cycles for NiWO₄/Ni foam and CoWO₄/Ni foam, respectively. These outstanding electrochemical performances can be attributed to the excellent conductivity and high stability of the electrodes' material, reduced electro- and ion- transport pathways and enlarged contacting area with the electrolyte. The synthesis of other nanostructures of NiWO₄, CoWO₄ and their composites with other active materials on different current collectors and the fabrication of supercapacitor devices with multi-functional properties in ongoing.

Acknowledgements

G. J. He and J. M. Li contributed equally to this work. G. J. He would like to thank the University College London and China Scholarship Council for the joint PhD scholarship. Dr. Steve Firth, Mr. Martin Vickers and Dr. Qian Liu are acknowledged for their assistance in this work.

References

- 1 P. Simon and Y. Gogotsi, *Nat. Mater.*, 2008, **7**, 845.
- 2 W. W. Liu, C. X. Lu, X. L. Wang, K. Liang, B. K. Tay, *J. Mater. Chem. A*, 2015, **3**, 624.
- 3 J. H. Kim, K. Zhu, Y. F. Yan, C. L. Perkins and A. J. Frank, *Nano Lett.*, 2010, **10**, 4099.

- 4 Q. Yang, Z. Y. Lu, T. Li, X. M. Sun and J. F. Liu, *Nano Energy*, 2014, **7**, 170.
- 5 D. Z. Kong, J. S. Luo, Y. L. Wang, W. N. Ren, T. Yu, Y. S. Luo, Y. P. Yang and C. W. Cheng, *Adv. Funct. Mater.*, 2014, **24**, 3815.
- 6 S. Cong, Y. Y. Tian, Q. W. Li, Z. G. Zhao and F. X. Geng, *Adv. Mater.*, 2014, **26**, 4260.
- 7 D. H. Nagaraju, Q. Wang, P. Beaujuge and H. N. Alshareef, *J. Mater. Chem. A*, 2014, **2**, 17146.
- 8 C. H. An, Y. J. Wang, Y. N. Huang, Y. N. Xu, L. F. Jiao and H. T. Yuan, *Nano Energy*, 2014, **10**, 125.
- 9 G. Q. Zhang and X. W. Lou, *Adv. Mater.*, 2013, **25**, 976.
- 10 L. Q. Mai, F. Yang, Y. L. Zhao, X. Xu, L. Xu and Y. Z. Luo, *Nat. Commun.*, 2011, **2**, 381.
- 11 S. J. Peng, L. L. Li, H. B. Wu, S. Madhavi and X. W. Lou, *Adv. Energy Mater.* 2014, 1401172.
- 12 L. Zhou, D. Y. Zhao and X. W. Lou, *Adv. Mater.*, 2012, **24**, 745.
- 13 T. Peng, Z. Qian, J. Wang, D. Song, J. Liu, Q. Liu and P. Wang, *J. Mater. Chem. A*, 2014, **2**, 19376.
- 14 H. Chen, J. Jiang, L. Zhang, H. Wan, T. Qi and D. Xia, *Nanoscale*, 2013, **5**, 8879.
- 15 Y. Bi, H. Nie, D. Li, S. Zeng, Q. Yang and M. Li, *Chem. Commun.*, 2010, **46**, 7430.
- 16 B. Sun, W. Zhao, L. Wei, H. Li and P. Chen, *Chem. Commun.*, 2014, **50**, 13142.
- 17 S. Rajagopal, D. Nataraj, O. Y. Khyzhun, Y. Djaoued, J. Robicchaud and D.

- Mangalaraj, *J. Alloys Comp.*, 2010, **493**, 340.
- 18 L. Y. Niu, Z. P. Li, Y. Xu, J. F. Sun, W. Hong, X. H. Liu, J. Q. Wang and S. R. Yang, *ACS Appl. Mater. Interfaces*, 2013, **5**, 8044.
- 19 R. Bharati, R. A. Singh, *J. Mater. Sci.*, 1983, **18**, 1540.
- 20 B. Moreno, E. Chinarro, M. T. Colomer and J. R. Jurado, *J. Phys. Chem. C*, 2010, **114**, 4251.
- 21 P. K. Pandey, N. S. Bhawe and R. B. Kharat, *Mater. Res. Bull.*, 2006, **41**, 1160.
- 22 J. Yan, T. Wang, G. Wu, W. Dai, N. Guan, L. Li and J. Gong, *Adv. Mater.*, 2015, **27**, 1580.
- 23 U. M. García-Pérez, A. Martínez-de la Cruz and J. Peral, *Electrochim. Acta*, 2012, **81**, 227.
- 24 Y. F. Bi, H. Nie, D. D. Li, S. Q. Zeng, Q. H. Yang and M. F. Li, *Chem. Commun.*, 2010, **46**, 7430.
- 25 X. W. Xu, J. F. Shen, N. Li and M. X. Ye, *Electrochim. Acta*, 2014, **23**, 150.
- 26 Y. J. Cao, W. Y. Li, K. B. Xu, Y. X. Zhang, T. Ji, R. J. Zou, J. M. Yang, Z. Y. Qin and J. Q. Hu, *J. Mater. Chem. A*, 2014, **2**, 20723.
- 27 W. Y. Li, G. Li, J. Q. Sun, R. J. Zou, K. B. Xu, Y. G. Sun, Z. G. Chen, J. M. Yang and J. Q. Hu, *Nanoscale*, 2013, **5**, 2904.
- 28 V. H. Nguyen and J. J. Shim, *J. Power Source*, 2015, **110**, 2730.
- 29 M. N. Mancheva, R. S. Iordanova, D. G. Klissurski, G. T. Tyuliev and B. N. Kunev, *J. Phys. Chem. C*, 2007, **111**, 1101.
- 30 L. Wang, H. Tian, D. L. Wang, X. J. Qin and G. J. Shao, *Electrochim. Acta*, 2014,

151, 407.

31 J. C. Deng, L. T. Kang, G. L. Bai, Y. Li, P. Y. Li, X. G. Liu, Y. Z. Yang, F. Gao and W. Liang, *Electrochim. Acta*, 2014, **132**, 127.

32 L. Gao, X. F. Wang, Z. Xie, W. Song, L. Wang, X. Wu, F. Qu, D. Chen and G. Z. Shen, *J. Mater. Chem. A*, 2013, **1**, 7167.

33 J. Yan, Z. J. Fan, W. Sun, G. Q. Ning, T. Wei, Q. Zhang, R. F. Zhang, L. J. Zhi and F. Wei, *Adv. Funct. Mater.*, 2012, **22**, 2632.

34 U. Nithiyantham, S.R. Ede, S. Anantharaj and S. Kundu, *Cryst. Growth Des.*, 2015, **15**, 673.

35 Y. H. Wang, C. C. Wang, W. Y. Cheng and S. Y. Lu, *Carbon*, 2014, **69**, 287.

36 G. H. Jeong, H. M. Lee, J. G. Kang, H. Lee, C. K. Kim, J. H. Lee, J. H. Kim and S. W. Kim, *ACS Appl. Mater. Interfaces*, 2014, **6**, 20171.

One pot synthesis of Nickel foam supported self-assembly of NiWO₄, CoWO₄ nanostructures that act as high performance electrochemical capacitor electrodes

Guanjie He^a, Jianmin Li^b, Wenyao Li^c, Bo Li^d, Nuruzzaman Noor^a, Kaibing Xu^b, Junqing Hu^{b*} and Ivan P. Parkin^{a*}

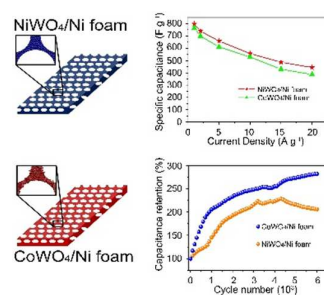
^a*Materials Chemistry Centre, Department of Chemistry, University College London, 20 Gordon Street, London WC1H 0AJ, U.K., E-mail: i.p.parkin@ucl.ac.uk*

^b*State Key Laboratory for Modification of Chemical Fibers and Polymer Materials, College of Materials Science and Engineering, Donghua University, Shanghai 201620, China. E-mail: hu.junqing@dhu.edu.cn*

^c*School of Material Engineering, Shanghai University of Engineering Science, Shanghai 201620, China*

^d*Department of Chemistry, Duke University, NC 27708, U.S.A.*

Graphical Abstract



Novel NiWO₄ and CoWO₄ nanostructures showed excellent electrochemical properties for supercapacitor electrodes, better than previously reported for these materials.